

Article

Power and Energy Management Strategies for a Microgrid with the Presence of Electric Vehicles and CAES Considering the Uncertainty of Resources

Reza Doosti, Alireza Rezazadeh * and Mostafa Sedighzadeh

Faculty of Electrical Engineering, Shahid Beheshti University, Evin, Tehran 983969411, Iran

* Correspondence: a-rezazade@sbu.ac.ir

Abstract: We are witnessing the growth of microgrid technology and the development of electric vehicles (EVs) in the world. These microgrids seek demand response (DR) and energy storage for better management of their resources. In this research, microgrids, including wind turbines, photovoltaics, battery charging/discharging, and compressed air energy storage (CAES), are considered. We will consider two scenarios under uncertainty: (a) planning a microgrid and DR without considering CAES, and (b) planning a microgrid and DR considering CAES. The cost of charging the battery in the second study decreased by \$0.66 compared to the first study. The battery is charged with a difference of \$0.7 compared to the case of the first study. We will also pay for unsupplied energy and excess energy in this microgrid. Then, we test the scheduling of vehicles to the grid (V2G) in the IEEE 33-bus network. The first framework for increasing network flexibility is the use of EVs as active loads. The scheduling of vehicles in the IEEE 33-bus network is simulated. Every hour, plug-in hybrid electric vehicle (PHEV) charging and discharging, active power loss, and cost will be compared with IHS and PSO algorithms. The difference obtained using the IHS algorithm compared to the PSO algorithm is 1.002 MW and the voltage difference is 9.14 pu.

Keywords: microgrid; energy management; V2G; compressed air energy storage; uncertainty of resources



Citation: Doosti, R.; Rezazadeh, A.; Sedighzadeh, M. Power and Energy Management Strategies for a Microgrid with the Presence of Electric Vehicles and CAES Considering the Uncertainty of Resources. *Processes* **2023**, *11*, 1156. <https://doi.org/10.3390/pr11041156>

Academic Editors: Chang-Hua Lin, Shiue-Der Lu and Hwa-Dong Liu

Received: 7 March 2023

Revised: 29 March 2023

Accepted: 30 March 2023

Published: 10 April 2023



Copyright: © 2023 by the authors. Licensee MDPI, Basel, Switzerland. This article is an open access article distributed under the terms and conditions of the Creative Commons Attribution (CC BY) license (<https://creativecommons.org/licenses/by/4.0/>).

1. Introduction

1.1. General Perspective

If energy consumption and management are not planned, losses and costs will increase [1,2]. Multiple-energy systems are the newest approach to planning energy systems [3,4]. These systems can meet different energy needs. The equipment required for this energy includes converters, storage, heating and cooling units, CHP, and electric vehicles [5]. The fields of energy planning, management, and optimization, have received more attention [6,7]. We describe studies in the field of energy hubs, electric vehicles, compressed air energy storage, and demand response.

1.2. Review of Recent Literature

In ref. [8], the authors provide power flow equations in multicarrier systems. The study and modeling of the energy hub can be seen in ref. [9]. The goals raised in the discussions of optimization in the field of energy have been to achieve economic exploitation. In addition, cases such as [10,11] also lead to the reduction in environmental pollutants. In [12], the design of the equipment used in the energy hub has been discussed. In [13], the authors presented a nonlinear method for optimal performance analysis. In [14], modeling for the use of multiple-energy carrier systems inside buildings is presented based on the concept of an energy hub. In [15] and its supplement [16], the authors presented a two-level control strategy for the on and off-time scheduling of units. The microgrid-based building management system under hub energy can be found in [17].

Uncertainty in the input data of the problem (load amount and energy price) is used in [18] to exploit the robust optimization method. In [19], a real-time energy system for EVs using prioritization is presented. In this system, energy optimization that integrates the dynamic charging system of the electric vehicle is a priority.

EV charging and discharging management for the operation of photovoltaic systems with grid coordination is discussed in [20]. In [21], EV charging stations are modeled and planned using spatial information systems. A fuzzy model of electric vehicles and optimal scheduling of distributed generation resources is proposed in [22]. In [23,24], solar charging stations for grid-connected electric vehicles are introduced. In addition, the MPPT technique is used to receive power from solar panels.

In [25], the management of electric vehicles in a smart grid for optimization and control has been investigated. In [26], the amount of energy exchanged between the distribution network and the electric vehicle is investigated. The concept of transferring electric energy from vehicle-to-grid (V2G) is related to the storage capability of electric vehicles. (Figure 1) shows the relationship between the factors of the smart grid model. The two-way flow of power is provided between the vehicle and the power grid.

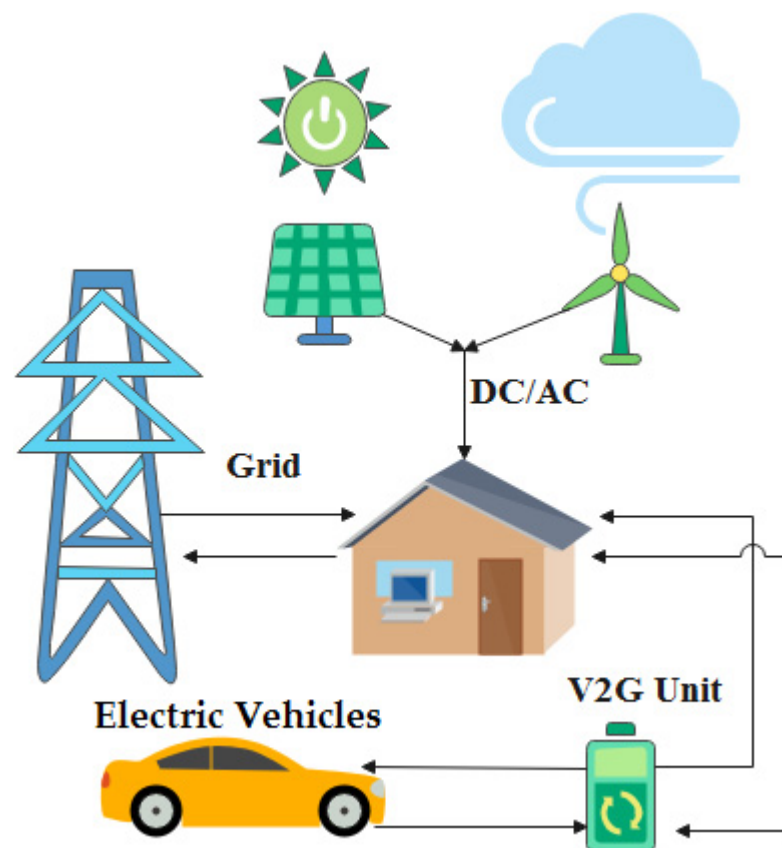


Figure 1. Transmission of electrical energy from vehicle-to-grid (V2G).

Furthermore, it provides better management of renewable energy resources that have high uncertainty. Using this feature improves flexibility and increases the reliability of the network [27]. Using V2G, the state of charge (SOC) of each electric vehicle's battery can be increased or decreased based on customer demand, network load, and profit from vehicle participation. Through the V2G feature, electric vehicles can earn money while their cars are parked, which could be a good incentive to move toward this scheme. In addition, by using V2G, network operators can overcome the uncertainty of sources (wind and solar energy) and improve the operating conditions of the network. In [28], the economic evaluation of CAES with wind turbines is considered. In the results of this reference, it can be seen that CAES has filled this gap well and increased its reliability. In [29], CAES has

been used as a compensator to increase the efficiency of the current passing through the distribution lines in the presence of a wind turbine. Stabilizing the operation of wind power plants in the event of a fault in the network is provided. The results show that the power system has passed the grid faults with enough stability. In [30], the authors have addressed the risk-limited strategy for building a CAES power plant. With the technical and economic studies of this plan, CAES can reduce losses and increase efficiency. In [31], modeling and experimental testing of a wind turbine system with CAES have been reviewed and analyzed. When wind turbine power fluctuates, CAES is a supplement to this process and increases reliability. Further, the results show that this design has reduced blackouts and increased power system efficiency. In [32], an economic evaluation suggested that CAES can increase energy efficiency by up to 90% with wind turbines, solar, and electric vehicles. In ref. [33], the mathematical modeling of electric vehicle contributions to the voltage security of smart distribution networks is carried out and the evaluation of the security of electrical energy distribution networks in the presence of electric vehicles is performed in [34]. Hybrid stochastic/robust flexible and reliable scheduling of secure networked microgrids with electric springs and electric vehicles is discussed in [35]. Exploring potential storage-based flexibility gains of electric vehicles is the topic of [36]. Storage-integrated virtual power plants for the resiliency enhancement of smart distribution systems is explored in [37], and network flexibility regulation by renewable energy hubs using flexibility pricing-based energy management is studied in [38].

DR is a set of measures that are implemented to change the pattern of electricity consumption to improve the reliability of the network and prevent price jumps, especially during peak hours of the network [39]. In [40], DR programs in smart grids have been introduced, and the effect of real-time pricing in smart grids has been studied. In [41], the effects of DR in the smart grid were investigated. In [42], intelligent energy management tools are reviewed, and noncritical load control programming in the residential sector is discussed. In [43], DR uses a standard function to improve the security of a microgrid and to provide a reservation system [44], and, finally, refs. [45,46] focuses on resource uncertainty management. In summary, the previous works can be specified in Table 1.

Table 1. Summary of previous works.

Reference	Electric Vehicles	CAES	DR	Energy Storage	Uncertainty Resources
[10]				✓	✓
[19]	✓			✓	
[28]		✓		✓	✓
[29]		✓			✓
[31]		✓			✓
[40]			✓	✓	
[44]			✓	✓	✓
suggested method	✓	✓	✓	✓	✓

1.3. Motivation and Structure of the Paper

In this article, the uncertainty of energy production systems (photovoltaic and wind), energy storage systems, and CAES communication links are used. The work of this article includes:

- Energy storage in microgrids considering the uncertainty of resources.
- Scenarios with and without CAES.
- Comparison of operating costs.
- Management strategy to achieve economic goals (surplus energy).
- Power planning and coordination between participating units.

- Selection of the IEEE 33-bus network for large systems and the examination of how PHEVs are charged and discharged.
- Economic indicators and network users are compared using two algorithms, IHS and PSO.

This paper is structured as follows: Section 2 describes the electric vehicle; Section 3 formulates the problem; Section 4 describes the studied system; Section 5 presents the simulation results; finally, conclusions are made.

2. Electric Vehicle and CAES

From a technical point of view, energy storage systems can be divided based on the technology used in Figure 2.

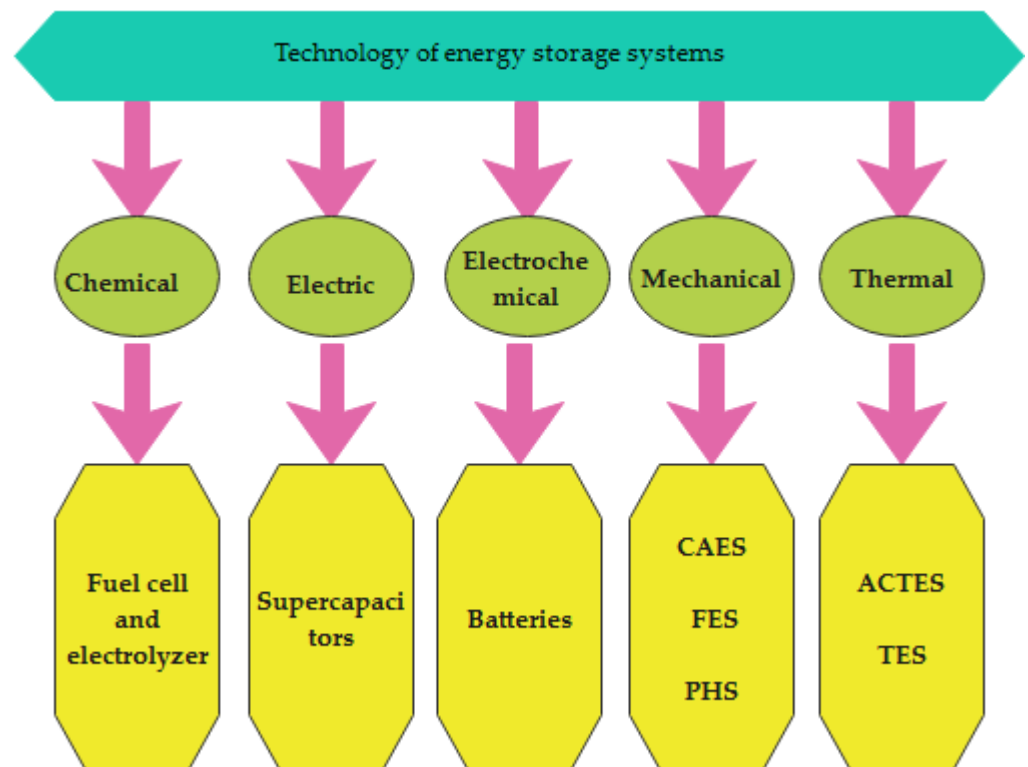


Figure 2. Types of energy storage systems.

ACTES in Figure 2 means thermal energy storage in air conditioning systems. Energy storage systems, PHS and CAES, have the highest energy storage capacity and can store energy for hours. The opinion is that high storage volume is the best option for use in network energy management or microgrids. One of the advantages of CAES is that you do not need to have a specific geographic shape to use it; however, the equipment required for this method must be installed in a large hollow space. One of the most important disadvantages is the use of CAES to store energy mechanically and then convert it back into electrical energy, because increasing the number of energy conversion cycles leads to a decrease in the efficiency of the entire storage system.

Regarding batteries, electric vehicles are used as storage for the microgrid. The working mechanism of these vehicles is that their batteries are charged during nonpeak hours, and when the vehicles are in the parking lot, the batteries are discharged, and power is injected back into the network during peak hours. Electric vehicles can operate in two modes: vehicle-to-grid (V2G) or grid-to-vehicle (G2V). Electric vehicle owners are encouraged to participate in the V2G program through certain incentives provided by smart parking management. SOC (state of charge) of the previous period ($SOC_v - t \Delta t$)

$$\alpha_s = \frac{\mu_s \times \beta_s}{(1 - \mu_s)} \quad (4)$$

where $f_b(si)$ is the beta density function, S is the random variable of solar radiation, Γ is the gamma function, μ and σ are the mean and standard deviation of sunlight, β is the shape factor, and α is the scale factor.

3.2. Wind Turbine

At moment t during 24 h when there is wind energy, the output power of each wind turbine is equal to [50,51]:

$$P_w(v) = \begin{cases} 0 & 0 \leq v \leq v_{ct} \\ P_{rated} \times \frac{(v-v_{ct})}{(v_r-v_{ct})} & v_{ct} \leq v \leq v_r \\ P_{rated} & v_r \leq v \leq v_{co} \\ 0 & v_{co} \leq v \end{cases} \quad (5)$$

where v is the wind speed and P_{rated} is the rated power of the wind turbine, v_{cut-in} and $v_{cut-out}$ is the speed of wind turbine, and v_r is the rated speed of the wind turbine.

3.3. Operation of Electric Vehicles

The following limitations represent the constraints of PEVs during two common mechanisms, which include the charging mechanism or G2V and the discharging mechanism or V2G [48].

$$\frac{P_{PEV,G2V}^{min}}{\eta_{G2V}} \times W_{G2V}(t) \times S_{trip}(t) \leq P_{PEV,G2V}(t) \leq \frac{P_{PEV,G2V}^{max}}{\eta_{G2V}} \times W_{G2V}(t) \times S_{trip}(t) \quad (6)$$

$$P_{PEV,V2G}^{min} \times \eta_{V2G} \times W_{V2G}(t) \times S_{trip}(t) \leq P_{PEV,V2G}(t) \leq P_{PEV,V2G}^{max} \times \eta_{V2G} \times W_{V2G}(t) \times S_{trip}(t) \quad (7)$$

where $P_{PEV,G2V}^{min}$ is the minimum power received from the network by vehicles, η_{G2V} is the charging efficiency of PEVs, $W_{G2V}(t)$ is the energy of PEVs from the grid, $S_{trip}(t)$ is the zero signal, $P_{PEV,G2V}(t)$ is the power of vehicles, $P_{PEV,G2V}^{max}(t)$ is the maximum power received from the network by vehicles, $P_{PEV,V2G}^{min}(t)$ is minimum power injected into the grid by vehicles, η_{V2G} is discharge efficiency of PEVs, $W_{V2G}(t)$ is energy injected by PVs into the grid, $P_{PEV,V2G}(t)$ is power injected into the grid by vehicles, and $P_{PEV,V2G}^{max}(t)$ is the maximum power injected into the network by vehicles. The zero signal ($S_{trip}(t)$) has already been announced by the owner of the electric vehicle to the operator of hub energy. When PEVs are available, the signal is zero-one and when they are unavailable, the signal is zero-zero. Electric vehicles in each interval t can only be in one of the G2V or V2G modes, and Equation (8) makes this constraint [48]:

$$W_{G2V}(t) + W_{V2G}(t) \leq 1 \quad (8)$$

The upper and lower limits of the capacity of electric vehicles are equal:

$$q_{PEV}^{min} \leq q_{PEV}(t) \leq q_{PEV}^{max} \quad (9)$$

The amount of energy stored in electric vehicles for the time interval $t \geq 1$ is determined according to Equation (10).

$$q_{PEV}(t) = q_{PEV}(t-1) + P_{PEV,G2V}(t) \times \eta_{G2V} \times \Delta t - \frac{P_{PEV,V2G}(t) \times \Delta t}{\eta_{V2G}}, t \geq 1 \quad (10)$$

To ensure that the amount of energy stored in electric vehicles reaches its initial value at the end of the planning period, the following constraint is defined [48]:

$$\eta_{G2V} \times \sum_{t=T} P_{PEV,G2V}(t) \times \Delta t = \frac{\sum_{t=T} P_{PEV,V2G}(t) \times \Delta t + q_{arrival}}{\eta_{V2G}} \quad (11)$$

To guarantee the maximum energy of electric vehicles when leaving the building, the following constraint must be observed:

$$q_{PEV}(t_d) = q_{PEV}^{max} \quad (12)$$

3.4. Constraints of Energy Storage Systems

When the output power of photovoltaic panels and wind generators is more than the load energy, the battery bank will be charging. The charge amount of the battery bank at the moment t is also calculated as follows [4]:

$$E_{Bat}(t) = E_{Bat}(t-1) * (1 - \sigma) + [(E_{PV}(t) + E_{WT}(t)) - (\frac{E_{load}(t)}{\eta_{Inv}})] \quad (13)$$

$E_{Bat}(t)$, $E_{Bat}(t-1)$ are the amounts of battery charge at moments t and $t-1$, respectively; σ is the hourly self-discharge rate; η_{Inv} is inverter efficiency; and E_{load} is load demand.

$$E_{Bat}(t) = E_{Bat}(t-1) * (1 - \sigma) + \left(\frac{E_{load}(t)}{\eta_{Inv}} - E_{PV}(t) + E_{WT}(t) \right) \quad (14)$$

3.5. Operation Costs

The operating cost of the storage battery in charging mode is calculated using Equation (15) [5]:

$$C_t^{B,charge} = \left(\frac{\frac{C_{in}^B}{L_t^{B,charge}} + C_{o\&M}^B}{\eta_{charge}^B \eta_{dcharge}^B} \right) * U_t^{charge} \quad (15)$$

where C_{in}^B and $C_{o\&M}^B$ are the investment cost and maintenance cost of the storage battery, and $L_t^{B,charge}$ is the useful life of the battery in charging mode (U_t^{charge} is rated voltage). The operating cost of the storage battery in discharge mode is calculated using Equation (16):

$$C_t^{B,discharge} = \left(\frac{C_{in}^B}{L_t^{B,discharge}} + C_{o\&M}^B \right) * U_t^{discharge} \quad (16)$$

3.6. PSO and IHS Algorithm

In this section, we briefly discuss these algorithms.

In the PSO algorithm [52,53], the population has n particles that represent candidate responses.

Each particle is a real-valued m -dimensional vector, where m is the number of optimized parameters; therefore, each optimized parameter represents a dimension of the problem space. The PSO technique can be described as the following steps:

Step 1: (Initialization): Set the timer to $t = 0$ and generate n random chromosomes.

$[x_j(0), j = 1, \dots, n]$, where $x_j(0) = [x_{j,1}(0), x_{j,2}(0), \dots, x_{j,m}(0)]$. $x_{j,k}(0)$ is generated in each state space $[x_{kmin}, x_{kmax}]$. $V_j(0)$ is generated to test the objective function.

For each particle, set $x_j^*(0) = x_j(0)$ and $j^*j = jj, j = 1, 2, \dots, n$.

Step 2: (time update): update the time counter $t = t + 1$.

Step 3: (Weight Update): update the inertial weight.

Step 4: (velocity update): an update using the global best and the individual best, and the particle velocity uses Eqs.

Step 5: (update the position): Based on the updated speed, each particle has its own position. If the particle exceeds its positional limits in any dimension, adjust its position to its appropriate limits.

Step 6: Each particle is evaluated according to its updated position.

Step 7: Now find the minimum value.

Step 8: If one of the stop conditions is met, then stop; otherwise, go to step 2.

Improved harmony search (IHS) [54] is a powerful search algorithm to find optimal solutions. In the production of a piece of music, several musicians collaborate with different instruments. Their goal is to produce beautiful music. In this process, everyone tries to choose more suitable notes every time they play music so that better music can be created. In fact, the beauty of music gets better with its production. In general, the process of music production attempts to make the music evolve more in each stage of the performance if in the end there is proper harmony between the musicians. Over time, these musicians produce a piece of music by playing different harmonies. After playing several pieces, these musicians remember the pieces played (the harmonies of that piece). Suppose that k harmonies are composed by n musicians, it is assumed that the musicians' memory size, or (HMS), is equal to k harmonies.

So according to the following relationship, a matrix with k rows (the number of harmonies that the musicians remember) and $n + 1$ columns where n is the number of musicians (the number of influencing variables in the problem = n) and one column for the value of that harmony ($f(x)$) is considered.

This algorithm consists of five steps:

1. Initialization of the optimization problem and initial parameters.
2. Setting the harmonious memory.
3. Creating a new and improved harmony.
4. Updating the harmonious memory.
5. Repeating steps 3 and 4 until the final condition is satisfied or the repetitions are finished.

4. The System under Test

For the effectiveness of the proposed method in this section, energy management includes wind turbines, solar cells, storage batteries, and CAES. The simulation was performed using MATLAB software. Two studies are considered:

1. Planning a microgrid DR without considering CAES;
2. Planning a microgrid and DR considering CAES.

After the above two studies, we tested the design on the IEEE 33-bus system. The costs from the power company, active power losses, and bus voltage deviations at different hours of the day and night are shown on different buses. The information on the studied system can be seen in Tables 2–5.

Table 2. Wind turbine parameters.

Wind Turbine	
Parameter	Value
P_{rated} (kW)	3
v_r (m/s)	14
v_{co} (m/s)	25
v_{ct} (m/s)	2

Table 3. Solar cell parameters.

Solar Cell	
Parameter	Value
$P_{rated} (w)$	220
η^{pv}	18.1
Open circuit voltage	22.9
The maximum power voltage	26.3
Short circuit current	8.21

Table 4. Storage battery parameters.

Storage Battery	
Parameter	Value
$P_{rated} (w)$	12
Rated capacity (Ah)	240
Number of batteries	32
SOC^{max}	90%
SOC^{min}	60%
$SOC^{initial}$	80%
$P_{charge(max)}$	180
$P_{charge(min)}$	0
η_{charge}^B	82%
$\eta_{diccharge}^B$	90%

Table 5. CAES parameters.

CAES	
Parameter	Value
$P_{rated} (w) (max)$	6.2 kW
$P_{rated} (w) (min)$	1.5 kW
η^H	50%
η^{FC}	40%
P_{max}^{FC}	6 kW
P_{min}^{FC}	0.5 kW

5. Simulation Results

In this section, we examine the simulation results of the proposed model. The base load curve of the system is shown in Figure 4. This curve is divided into three separate periods: low load from 1 to 8, medium load from 9 to 14 and 22 to 24, and peak load from 15 to 19.

The power produced by the wind turbine and the solar cell over 24 h is shown in Figures 5 and 6, respectively. Figure 7 shows the microgrid load considering the DR for the two studied systems. We obtain the operation cost of the entire microgrid through this graph. These results are given in Table 6. The comparative results for different costs including battery cost, CAES, unsupplied energy, surplus energy, and total operating cost are presented. In the second study, it can be seen that the total operating cost of the microgrid has decreased significantly with the presence of the CAES. Figures 8 and 9 show the unsupplied energy and surplus energy for different hours of the day and night in the studied mode, respectively (the energy surplus occurs after passing through the peak load after 22:00).

According to the table and figures, it can be seen that CAES leads to a significant reduction in excess cost and energy supply.

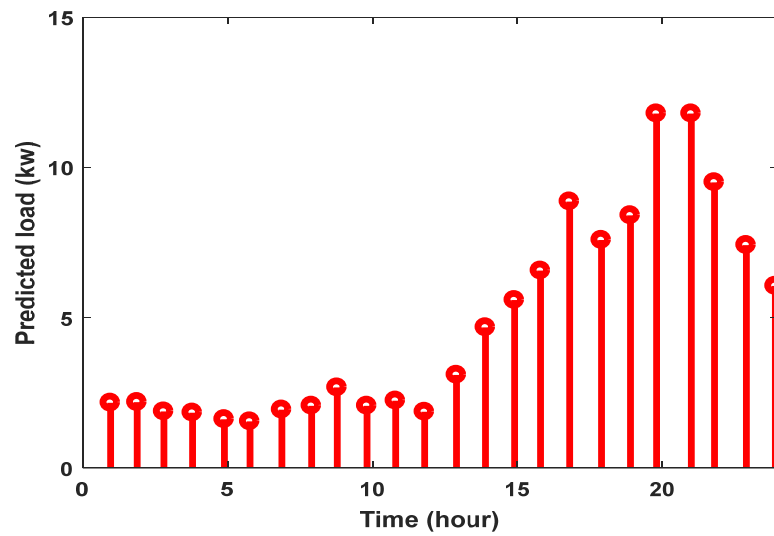


Figure 4. The load of the studied microgrid.

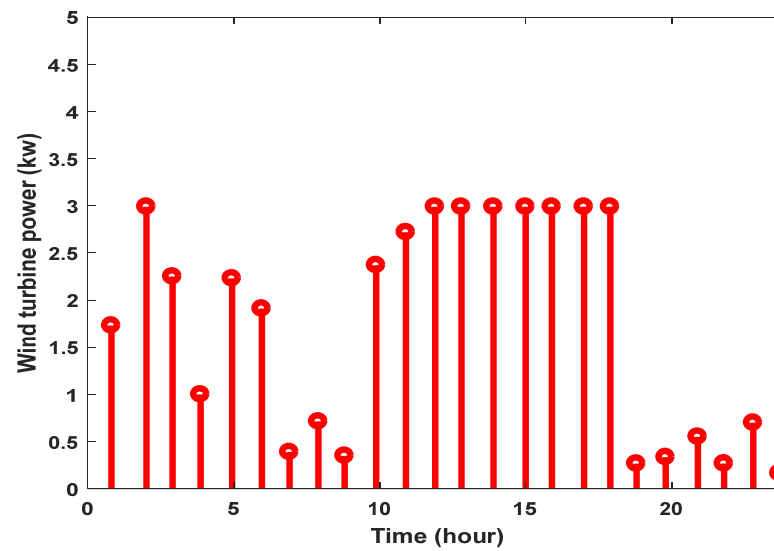


Figure 5. The power produced by the wind turbine with maximum operating power.

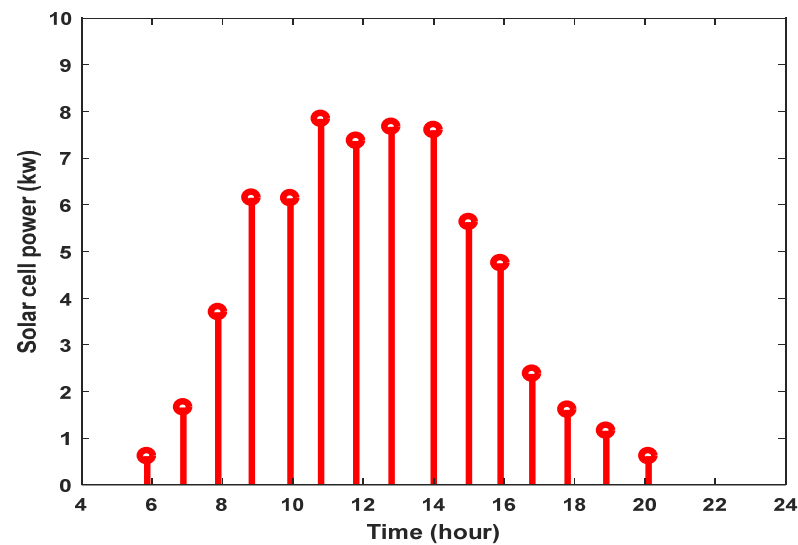


Figure 6. The power production of the solar system with maximum operating power.

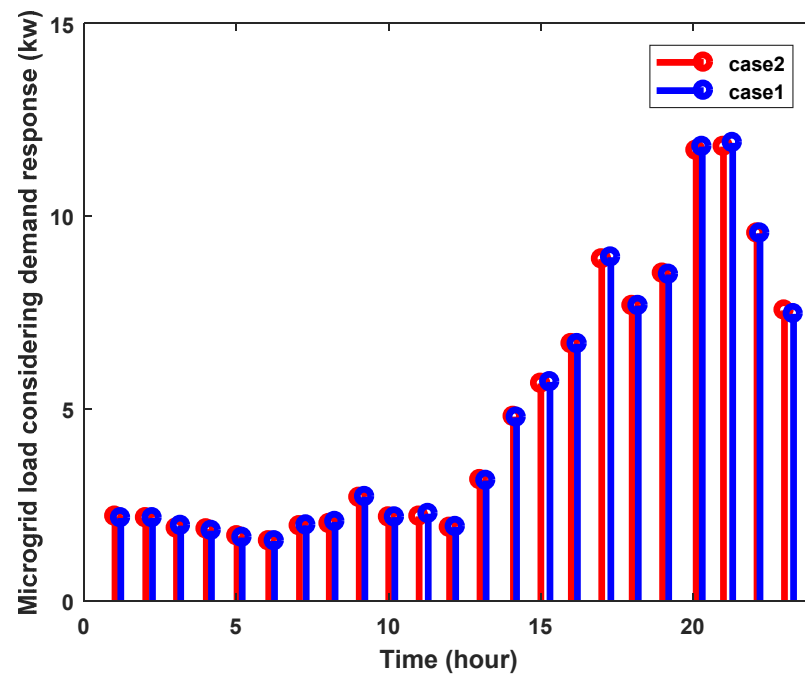


Figure 7. Microgrid load considering DR.

Table 6. Comparison of operating costs.

Costs (\$)	The First Study	The Second Study
The cost of charging the battery	6.30	5.64
The cost of discharging the battery	5.81	5.11
The cost of charging CAES	0	76.20
The cost of discharging CAES	0	7.52
Unsupplied energy costs	176.14	161.24
Surplus energy cost	142.25	9.21
Total cost of operation	330.50	264.92

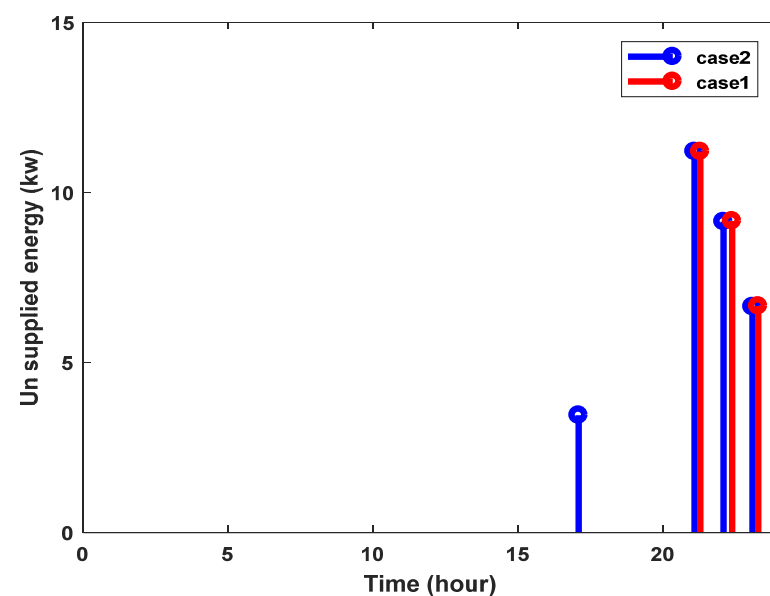


Figure 8. Unsupplied energy for the two studied systems.

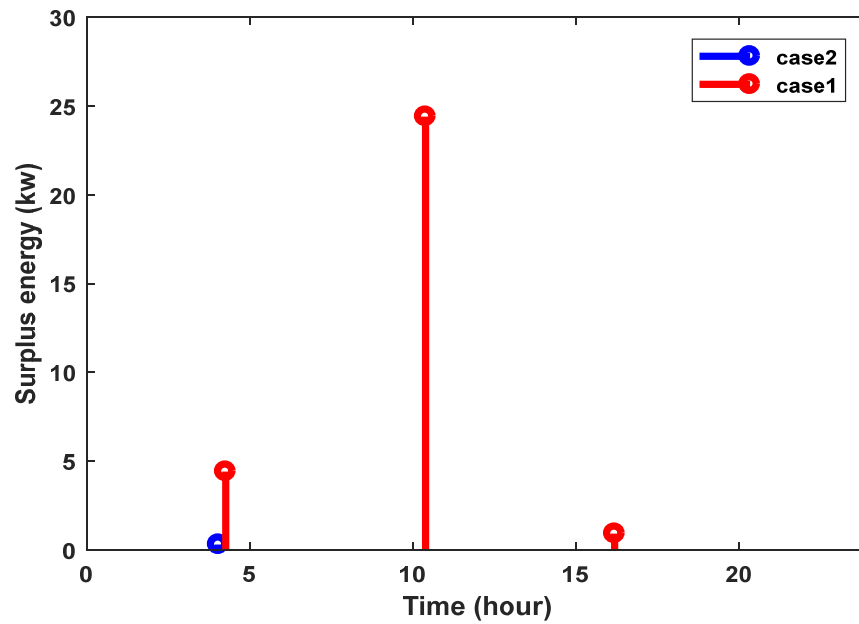


Figure 9. Surplus energy for the two studied systems.

The charge and discharge curves of the battery are shown in Figure 10 and the amount of energy stored in the storage battery is shown in Figure 11. Figure 12 shows the amount of pressure stored in the CAES, according to which, the second system has more storage than the first. The total operating cost in the first study is \$330.50 and in the second study, this amount is reduced to \$264.92. The cost of charging the battery in the second study decreased by \$0.66 compared to the first study. In the second study, the battery is charged with a difference of \$0.7 compared to the first case.

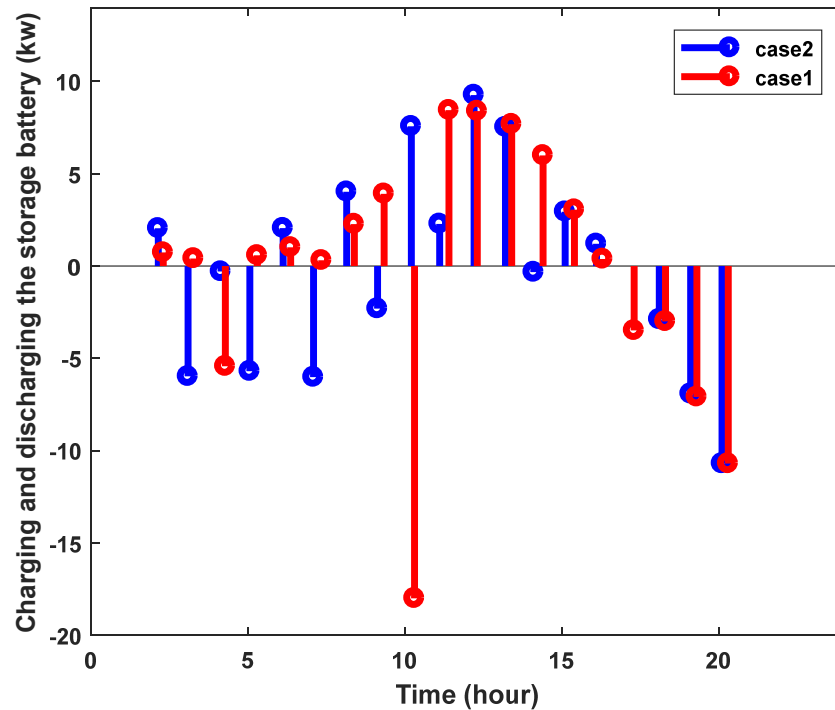


Figure 10. Charge and discharge curve.

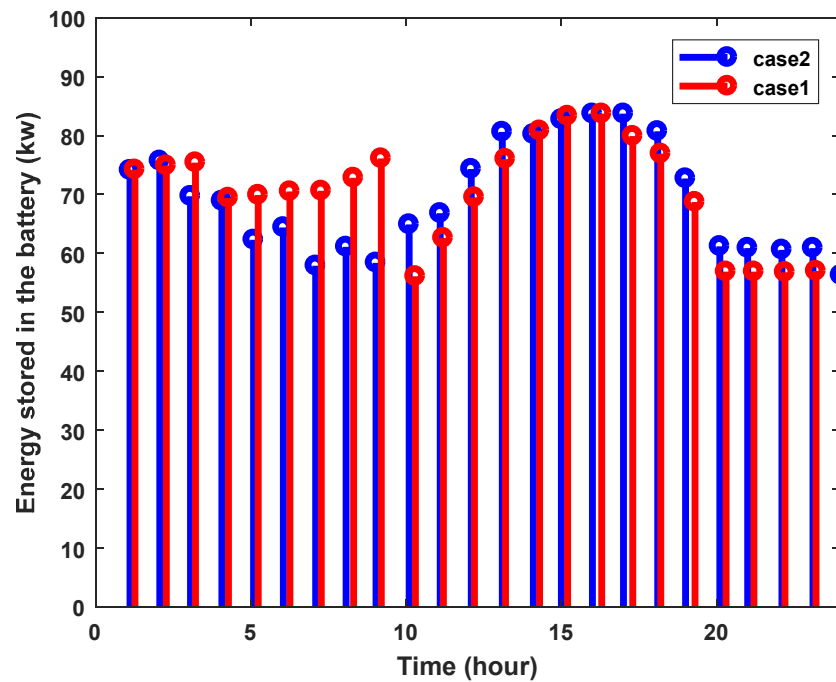


Figure 11. The amount of energy stored in the battery.

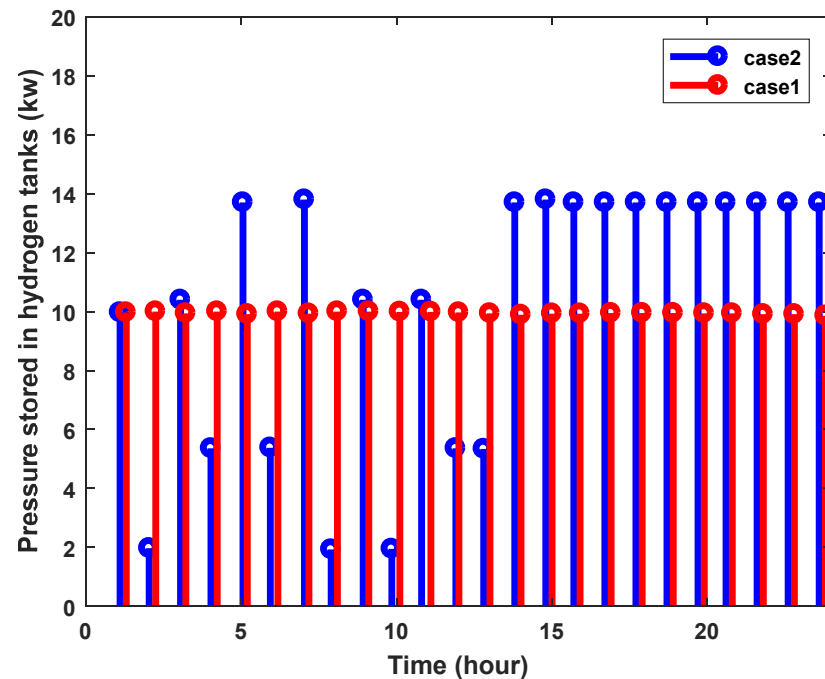


Figure 12. The amount of pressure stored in the CAES.

In this section, IEEE 33-bus system (Figure 13) is used for electric vehicles (V2G). In this paper, it is assumed that the capacity of each PHEV vehicle is equal to 1.8 kW, and 100 vehicles are considered on each bus. The cost of the power company, active power losses, and bus voltage deviations at different hours of the day and night are given in Table 7. These results have been compared using two algorithms, HIS and PSO. In the following, it can be seen that the difference is 1.002 MW and the voltage difference is 9.14 pu, which has a better result than the IHS algorithm. Table 8 shows the charging and discharging of vehicles connected to different buses of the network at different hours of the day and night.

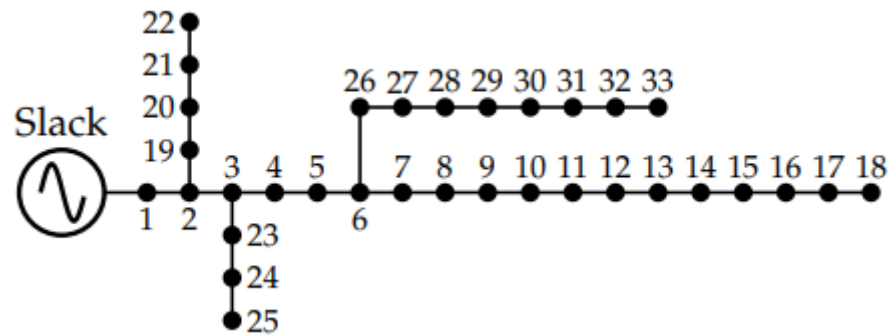


Figure 13. Structure of the IEEE 33-bus network.

Table 7. Economic indicators and network operation.

	The Cost of the Electricity Company (Dollars)	Daily Losses (MW)	Daily Voltage Deviation (PU)
IHS	1,448,985	5.216	40.88
PSO	-1,274,026	6.214	50.02

Table 8. Charging and discharging rate of PHEVs.

Hour	Bus 2	Bus 3	Bus 4	Bus 5	Bus 6	Bus 7	Bus 8	Bus 9
1	-0.203949	-0.04937	0.207117	0.072334	0.401745	0.163183	0.149927	0.124387
2	-0.24253	0.0729	-0.04012	0.263437	0.363042	0.173938	-0.01371	0.08419
3	0.01042	0.14861	-0.4001	0.110689	0.361972	-0.01498	0.0480303	0.042121
4	0.340911	0.484103	-0.18485	-0.30222	0.325129	0.16081	0.004849	-0.06615
5	0.065834	-0.49816	-0.39088	0.398001	0.2640030	0.107689	0.21215	0.079658
6	-0.07177	-0.21295	-0.06469	-0.3547	0	0.125458	0.016507	-0.19675
7	0.265884	0.191692	-0.16909	-0.40229	0	-0.03688	0.0335905	0.579884
8	-0.22318	0	-0.32062	0	0.419039	0	0	0
9	-0.37506	0	0.037676	0.13145	0.243154	0.17718	0.229969	-0.23253
10	0.371754	0.174604	-0.04403	-0.21709	0.554874	0.266126	0.090625	0
11	0.332572	0.409071	-0.23287	0.325205	0.32205	0.143872	0.391532	0.256686
12	0.176556	0	-0.31477	0.295431	0.295431	0.444412	0.107212	0.117152
13	0	0	0.18944	0.607727	0.607727	0	0.253204	0.30385
14	0.437693	-0.08883	-0.5498	0.44691	0.471066	0	0.460542	0.011372
15	-0.06834	0.268593	0	0.1408	0	0.345404	0.332172	-0.45478
16	-0.0286554	-0.06765	-0.06849	0.190355	0	0.031948	0	0.460968
17	-0.22902	0.031767	0	0.0187853	0.338051	0.174974	0.362333	0
18	-0.37536	0.152148	0.008893	0	0.283249	0.073157	0.254523	0
19	-0.00954	0	-0.10208	-0.26847	0.20972	0	0.238312	0.128627
20	0.287311	0	0.005446	-0.04548	0.370011	0.074291	-0.13023	-0.31137
21	0.090822	-0.19068	0.199705	-0.17544	0.341616	0	0.298338	0.263416
22	0.279221	0.045887	0.007725	-0.015	0.581751	0.01244	0.264084	0.016971
23	0.0460825	0.054172	0.250793	0.061933	0.501601	0.354406	0.359602	0.05852
24	-0.10182	-0.27968	0.145563	0.281277	0.340406	0.517129	0.372365	0.13524

Table 8. Cont.

Hour	Bus 10	Bus 11	Bus 12	Bus 13	Bus 14	Bus 15	Bus 16	Bus 17
1	−0.2172	−0.1151	0.340538	−0.28858	0.13397	0.215	0.509886	0.0296391
2	−0.48069	−0.29731	0.261252	0.228911	0.291982	−0.07889	0.747164	−0.1629
3	−0.30994	−0.11412	0.42172	0.082115	−0.05983	0.262531	0.433044	−0.19196
4	−0.02283	−0.38287	0.251726	0.025115	0.060952	0.000117	0.470921	0.592725
5	−0.04582	0.232496	0.266468	0.212757	0.242039	0.057211	0.636258	0.0373539
6	0.206411	−0.13927	0.162261	−0.28581	−0.2199	0.109305	0.494137	−0.1691
7	0	0	0	−0.05847	−0.29067	0.023746	0.564915	0.138637
8	0	0.499138	0.214762	−0.41379	0	−0.46763	0	−0.14096
9	0.41909	−0.1038	−0.15531	−0.01952	0.256453	0.219961	0	−0.00244
10	0.080388	0.030835	−0.03662	0.347494	−0.30092	−0.04624	0.343626	0
11	0.23086	−0.24074	0.574301	−0.10117	0	−0.22682	0.513629	−0.07183
12	−0.40219	0.019415	0.216366	0.179	0	0	0	−0.15631
13	−0.47158	−0.57507	0.143105	−0.01213	0.187238	0	0	0
14	−0.1416	0.033491	0.170398	0	0	0.135393	0.43174	0.420412
15	−0.19975	−0.14902	0	0	0.140293	−0.03003	0.523137	0.123951
16	−0.43673	−0.01715	0.031523	0	0.0323822	0	0.354602	0
17	−0.28284	0	0	0.007066	−0.10133	0	0.51713	0
18	0	0	0.225536	−0.30457	0	0	0	0
19	−0.25187	0.051541	0.022455	0.180663	0	0.192109	0.673497	0.33373
20	−0.07334	−0.41833	0.586493	0.151788	0.357167	0.392503	0.404807	−0.25816
21	−0.03598	0.002444	0.171143	−0.20991	0.245613	0.119169	0.55136	−0.09427
22	−0.10944	−0.13339	0.34417	−0.11676	−0.01339	0.056928	0.512181	−0.45705
23	−0.178767	0.067427	0.357452	0.185385	0.121004	0.048119	0.723733	0.531025
24	−0.02946	0.211197	0.08026	−0.08251	−0.00704	0.30513	−0.08473	0.402817
Hour	Bus 18	Bus 19	Bus 20	Bus 21	Bus 22	Bus 23	Bus 24	Bus 25
1	0.651439	−0.05569	0.38926	0.261946	0.375847	−0.33155	−0.53184	−0.34245
2	0.586311	0.107974	−0.20054	−0.00791	0.258296	−0.23722	−0.37175	−0.36514
3	0.491395	−0.04992	−0.30449	0.09066	0.407295	0.046916	−0.40595	−0.28248
4	0.312905	−0.21274	−0.2545	0.168318	0.383174	−0.08508	−0.48565	−0.43131
5	0.358369	−0.35149	−0.37688	−0.0402	0.288562	−0.14052	−0.28618	−0.32766
6	0.444779	−0.31761	−0.31283	0	0	0	−0.43382	−0.57932
7	0.282577	0.151033	0	0.262387	0	−0.27239	−0.48589	−0.44734
8	0	−0.26157	0	0.037639	0	0	−0.27377	−0.44177
9	0.369557	−0.24129	−0.17753	0.165351	0.512028	−0.34309	−0.41525	0
10	0.469584	0	−0.56927	−0.08343	0.63421	−0.13411	−0.40694	−0.34227
11	0.330625	0	−0.18361	−0.14442	0.155257	−0.340301	−0.489	−0.59589
12	0.353939	0.340993	−0.3735	0	0.492698	−0.23288	−0.47008	0
13	0.651421	−0.36893	−0.36278	0.0901198	0.44566	0	0	−0.037478
14	0.401976	−0.36893	−0.31686	−0.11612	0.247802	0	−0.50581	0
15	0.466945	0.156724	−0.19768	0.164742	0.040224	−0.35577	−0.62309	−0.36613

Table 8. Cont.

16	0.214875	0.357695	−0.06306	0.104369	0	0	0	−0.46353
17	0	0.372549	0	0.118784	0	−0.31297	−0.46577	−0.530547
18	0.448936	0.373463	0	0	0.351668	−0.11008	−0.39909	0
19	0.378952	−0.20447	−0.22115	0	−0.0009	−0.33243	−0.32844	0.38857
20	0.60299	−0.08439	−0.35351	−0.28189	0.434581	−0.385	−0.73094	−0.6762
21	0.151932	−0.04669	−0.47751	0.002604	0.537381	−0.00567	−0.16216	−0.182205
22	0.31492	0.18192	−0.3046	−0.37766	0.008083	−0.20462	−0.19482	−0.23413
23	0.421401	0.18192	−0.17169	0.144835	0.260384	−0.15718	−0.35868	−0.46065
24	0.35647	−0.15452	0.226561	0.255988	0.023404	−0.46672	−0.3653	0.270348
Hour	Bus 26	Bus 27	Bus 28	Bus 29	Bus 30	Bus 31	Bus 32	Bus 33
1	0.428738	−0.01673	−0.2551	0.502791	0.237749	0.0241	0.16671	0.110723
2	0.313738	0.048147	−0.28766	0.440024	−0.08471	−0.0522	0.032277	−0.21656
3	0.394222	0.268914	−0.51718	0.043121	0.096542	0.274971	−0.08428	0.180439
4	0.438966	0.036082	−0.44733	0.153678	−0.46993	−0.30151	−0.2651	0.047526
5	0.443398	−0.13357	−0.54546	−0.01295	0.197977	0.103994	−0.17329	0.320062
6	0.38228	−0.42829	−0.53531	−0.0517	−0.27115	0.158869	−0.04302	0.11763
7	0.490751	0.177673	0	−0.1409	−0.01322	00	−0.26453	0.117637
8	0.350049	0	0	0.109954	0	0.169267	0	0.401753
9	0.408608	0	−0.52508	0.085141	0	−0.02846	−0.1121	−0.56215
10	0.386839	0	−0.2563	−0.0905	0	0.177404	−0.10418	−0.1031
11	0.227575	0.161259	−0.17463	0.090592	−0.17413	−0.10196	−0.09633	0.218871
12	0	−0.07162	−0.48442	0	−0.19635	−0.11147	0.340564	−0.05679
13	0	−0.42522	−0.67722	0.228503	−0.21542	−0.31411	0.131029	0.094435
14	0.547113	−0.03325	−0.29095	0.201797	0	0.330721	−0.099	−0.03332
15	0.127924	0	−0.19762	−0.03345	0	0.136872	0.13808	−0.31831
16	0.467619	0	−0.31258	−0.31073	0.056218	0	−0.36914	−0.07377
17	0.377401	−0.14891	0	−0.02462	0.207091	0	0	−0.08038
18	0.35931	0.006437	0	−0.19014	0.270689	−0.05019	0.406462	0
19	0.365355	−0.16547	−0.54107	0.248037	0	−0.29154	−0.02945	−0.22178
20	0.56139	0.060062	−0.35307	−0.16436	0	0.0627286	0.078289	0.1006
21	0.327704	0.055049	−0.67088	0.401693	−0.26853	0.05126	0.21737	0.023826
22	0.695965	−0.2506	−0.56763	0.053874	−0.34784	0.022541	0.161653	0.209788
23	0.449066	0.012106	−0.55343	0.206588	0	0.05905	−0.32029	0.064532
24	0.111256	−0.59539	−0.05267	0.392084	−0.30073	0.072399	−0.10285	−0.08514

6. Conclusions

One solution is to use distributed energy sources using existing infrastructure to meet electricity demand. In fact, the integration of energy operations may save energy resources as much as possible by optimally distributing energy between different consumers. An integrated energy system should be considered in different areas of management, planning, consumption, and optimization. In order to integrate the transmission, saving, and conversion of energy, a system called an energy hub is used, which applies to all carriers. Due to the use of different technologies of distributed generation sources and energy storage devices in the microgrid based on an energy hub, energy management can create many

challenges for the microgrid in the coming times. For this reason, a framework is presented to overcome some of these challenges in this study. In this research, we first focused on microgrid planning with the presence of wind and solar sources, energy storage, and CAES. As shown, the total operating cost is reduced compared to the first case with the presence of the CAES. Then we tested the scenario in the big IEEE 33-bus system. The results of charging and discharging vehicles cause the network load to change. PHEV charging and discharging planning has been performed in such a way that the vehicles are charged during off-peak hours and discharged during busy hours.

Future work includes:

1. Strategy and concurrent management of ACES load response, with new algorithms.
2. Using resources such as diesel generators in the model.
3. Power system models with many buses.

Author Contributions: Methodology, A.R.; Software, R.D.; Validation, A.R. and M.S.; Formal analysis, R.D.; Investigation, R.D.; Resources, A.R.; Data curation, M.S.; Writing—original draft, A.R. and M.S.; Supervision, M.S.; Project administration. All authors have read and agreed to the published version of the manuscript.

Funding: This research received no external funding.

Data Availability Statement: The data used in this study are reported in the paper's figures and tables.

Conflicts of Interest: The authors declare no conflict of interest.

References

1. Hirsch, A.; Parag, Y.; Guerrero, J. Microgrids: A review of technologies, key drivers, and outstanding issues. *Renew. Sustain. Energy Rev.* **2018**, *90*, 402–411. [[CrossRef](#)]
2. Grisales-Noreña, L.F.; Ocampo-Toro, J.A.; Rosales-Muñoz, A.A.; Cortes-Cañedo, B.; Montoya, O.D. An Energy Management System for PV Sources in Standalone and Connected DC Networks Considering Economic, Technical, and Environmental Indices. *Sustainability* **2022**, *14*, 16429. [[CrossRef](#)]
3. Maanavi, M.; Najafi, A.; Godina, R.; Mahmoudian, M.; Rodrigues, E.M.G. Energy Management of Virtual Power Plant Considering Distributed Generation Sizing and Pricing. *Appl. Sci.* **2019**, *9*, 2817. [[CrossRef](#)]
4. Zhu, W.; Guo, J.; Zhao, G. Multi-Objective Dispatching Optimization of an Island Microgrid Integrated with Desalination Units and Electric Vehicles. *Processes* **2021**, *9*, 798. [[CrossRef](#)]
5. Nazari-Heris, M.; Mirzaei, M.A.; Asadi, S.; Mohammadi-Ivatloo, B.; Zare, K.; Jebelli, H. A hybrid robust-stochastic optimization framework for optimal energy management of electric vehicles parking lots. *Sustain. Energy Technol. Assess.* **2021**, *47*, 101467. [[CrossRef](#)]
6. Aluisio, B.; Dicorato, M.; Forte, G.; Trovato, M. An optimization procedure for Microgrid day-ahead operation in the presence of CHP facilities. *Sustain. Energy Grids Netw.* **2017**, *11*, 34–45. [[CrossRef](#)]
7. Akbari, E.; Shafaghathian, N.; Zishan, F.; Montoya, O.D.; Giral-Ramirez, D.A. Optimized Two-Level Control of Islanded Microgrids to Reduce Fluctuations. *IEEE Access* **2022**, *10*, 95824–95838. [[CrossRef](#)]
8. Montoya, O.D.; Zishan, F.; Giral-Ramirez, D.A. Recursive Convex Model for Optimal Power Flow Solution in Monopolar DC Networks. *Mathematics* **2022**, *10*, 3649. [[CrossRef](#)]
9. Connolly, D.; Lund, H.; Mathiesen, B. Smart Energy Europe: The technical and economic impact of one potential 100% renewable energy scenario for the European Union. *Renew. Sustain. Energy Rev.* **2016**, *60*, 1634–1653. [[CrossRef](#)]
10. Pazouki, S.; Haghifam, M.-R. Optimal planning and scheduling of energy hub in presence of wind, storage and demand response under uncertainty. *Int. J. Electr. Power Energy Syst.* **2016**, *80*, 219–239. [[CrossRef](#)]
11. Ma, T.; Wu, J.; Hao, L. Energy flow modeling and optimal operation analysis of the micro energy grid based on energy hub. *Energy Convers. Manag.* **2017**, *133*, 292–306. [[CrossRef](#)]
12. del Real, A.J.; Arce, A.; Bordons, C. Optimization strategy for element sizing in hybrid power systems. *J. Power Source* **2009**, *193*, 315–321. [[CrossRef](#)]
13. Bilil, H.; Aniba, G.; Maaroufi, M. Probabilistic Economic Emission Dispatch Optimization of Multi-sources Power System. *Energy Procedia* **2014**, *50*, 789–796. [[CrossRef](#)]
14. Siano, P. Demand response and smart grids—A survey. *Renew. Sustain. Energy Rev.* **2014**, *30*, 461–478. [[CrossRef](#)]
15. Vytelingum, P.; Voice, T.D.; Ramchurn, S.D.; Rogers, A.; Jennings, N.R. Agent-based micro-storage management for the smart grid. In Proceedings of the 9th International Conference on Autonomous Agents and Multiagent Systems, Toronto, ON, Canada, 10–14 May 2010.

16. Akhil, A.A.; Huff, G.; Currier, A.B.; Hernandez, J.; Bender, D.A.; Kaun, B.C.; Rastler, D.M.; Chen, S.B.; Cotter, A.L.; Bradshaw, D.T.; et al. *DOE/EPRI 2013 Electricity Storage Handbook in Collaboration with NRECA*; Sandia National Laboratories: Albuquerque, NM, USA, 2013; Volume 1, p. 340.
17. Tighiz, L.; Yang, H.; Piran, M.J. A survey on enhanced smart micro-grid management system with modern wireless technology contribution. *Energies* **2020**, *13*, 2258. [[CrossRef](#)]
18. Becker, T.A.; Sidhu, I.; Tenderich, B. *Electric Vehicles in the United States: A New Model with Forecasts to 2030*; Center for Entrepreneurship and Technology, University of California: Berkeley, CA, USA, 2009; p. 24.
19. Lee, J.; Lee, H. A New HEV Power Distribution Algorithm Using Nonlinear Programming. *Appl. Sci.* **2022**, *12*, 12724. [[CrossRef](#)]
20. Almugham, O.; Ben Slama, S.; Zafar, B. Model for Managing the Integration of a Vehicle-to-Home Unit into an Intelligent Home Energy Management System. *Sensors* **2022**, *22*, 8142. [[CrossRef](#)]
21. Dominguez-Jimenez, J.; Campillo, J.; Montoya, O.; Delahoz, E.; Hernández, J. Seasonality Effect Analysis and Recognition of Charging Behaviors of Electric Vehicles: A Data Science Approach. *Sustainability* **2020**, *12*, 7769. [[CrossRef](#)]
22. Clement-Nyns, K.; Haesen, E.; Driesen, J. The impact of vehicle-to-grid on the distribution grid. *Electr. Power Syst. Res.* **2011**, *81*, 185–192. [[CrossRef](#)]
23. Dyke, K.J.; Schofield, N.; Barnes, M. The Impact of Transport Electrification on Electrical Networks. *IEEE Trans. Ind. Electron.* **2010**, *57*, 3917–3926. [[CrossRef](#)]
24. Tighiz, L.; Mansouri, S.; Zishan, F.; Yoo, J.; Shafaghathian, N. Maximum Power Point Tracking for Photovoltaic Systems Operating under Partially Shaded Conditions Using SALP Swarm Algorithm. *Energies* **2022**, *15*, 8210. [[CrossRef](#)]
25. Hartmann, N.; Özdemir, E. Impact of different utilization scenarios of electric vehicles on the German grid in 2030. *J. Power Source* **2011**, *196*, 2311–2318. [[CrossRef](#)]
26. Mohiti, M.; Monsef, H.; Lesani, H. A decentralized robust model for coordinated operation of smart distribution network and electric vehicle aggregators. *Int. J. Electr. Power Energy Syst.* **2018**, *104*, 853–867. [[CrossRef](#)]
27. Liu, C.; Chau, K.T.; Wu, D.; Gao, S. Opportunities and Challenges of Vehicle-to-Home, Vehicle-to-Vehicle, and Vehicle-to-Grid Technologies. *Proc. IEEE* **2013**, *101*, 2409–2427. [[CrossRef](#)]
28. Cleary, B.; Duffy, A.; O'Connor, A.; Conlon, M.; Fthenakis, V. Assessing the Economic Benefits of Compressed Air Energy Storage for Mitigating Wind Curtailment. *IEEE Trans. Sustain. Energy* **2015**, *6*, 1021–1028. [[CrossRef](#)]
29. Le, H.T.; Santoso, S. Operating compressed-air energy storage as dynamic reactive compensator for stabilising wind farms under grid fault conditions. *IET Renew. Power Gener.* **2013**, *7*, 717–726. [[CrossRef](#)]
30. Shafiee, S.; Zareipour, H.; Knight, A.M.; Amjady, N.; Mohammadi-Ivatloo, B. Risk-Constrained Bidding and Offering Strategy for a Merchant Compressed Air Energy Storage Plant. *IEEE Trans. Power Syst.* **2016**, *32*, 946–957. [[CrossRef](#)]
31. Krupke, C.; Wang, J.; Clarke, J.; Luo, X. Modeling and Experimental Study of a Wind Turbine System in Hybrid Connection With Compressed Air Energy Storage. *IEEE Trans. Energy Convers.* **2016**, *32*, 137–145. [[CrossRef](#)]
32. Li, N.; Hedman, K.W. Economic Assessment of Energy Storage in Systems With High Levels of Renewable Resources. *IEEE Trans. Sustain. Energy* **2014**, *6*, 1103–1111. [[CrossRef](#)]
33. Pirouzi, S.; Aghaei, J. Mathematical modeling of electric vehicles contributions in voltage security of smart distribution networks. *Simulation* **2019**, *95*, 429–439. [[CrossRef](#)]
34. Pirouzi, S.; Aghaei, J.; Shafie-Khah, M.; Osório, G.J.; Catalão, J.P.S. Evaluating the security of electrical energy distribution networks in the presence of electric vehicles. In Proceedings of the 2017 IEEE Manchester PowerTech, Manchester, UK, 18–22 June 2017; pp. 1–6.
35. Norouzi, M.; Aghaei, J.; Pirouzi, S.; Niknam, T.; Fotuhi-Firuzabad, M.; Shafie-Khah, M. Hybrid stochastic/robust flexible and reliable scheduling of secure networked microgrids with electric springs and electric vehicles. *Appl. Energy* **2021**, *300*, 117395. [[CrossRef](#)]
36. Pirouzi, A.; Aghaei, J.; Pirouzi, S.; Vahidinasab, V.; Jordehi, A.R. Exploring potential storage-based flexibility gains of electric vehicles in smart distribution grids. *J. Energy Storage* **2022**, *52*, 105056. [[CrossRef](#)]
37. Alayi, R.; Zishan, F.; Mohkam, M.; Hoseinzadeh, S.; Memon, S.; Garcia, D.A. A sustainable energy distribution configuration for microgrids integrated to the national grid using back-to-back converters in a renewable power system. *Electronics* **2021**, *10*, 1826. [[CrossRef](#)]
38. Akbari, E.; Shabestari, S.F.M.; Pirouzi, S.; Jadidoleslam, M. Network flexibility regulation by renewable energy hubs using flexibility pricing-based energy management. *Renew. Energy* **2023**, *206*, 295–308. [[CrossRef](#)]
39. Zishan, F.; Akbari, E.; Montoya, O.D.; Giral-Ramírez, D.A.; Nivia-Vargas, A.M. Electricity retail market and accountability-based strategic bidding model with short-term energy storage considering the uncertainty of consumer demand response. *Results Eng.* **2022**, *16*, 100679. [[CrossRef](#)]
40. Sheikhi, A.; Rayati, M.; Ranjbar, A.M. Demand side management for a residential customer in multi-energy systems. *Sustain. Cities Soc.* **2016**, *22*, 63–77. [[CrossRef](#)]
41. Wasilewski, J. Integrated modeling of microgrid for steady-state analysis using modified concept of multi-carrier energy hub. *Int. J. Electr. Power Energy Syst.* **2015**, *73*, 891–898. [[CrossRef](#)]
42. Saleem, M.U.; Usman, M.R.; Shakir, M. Design, Implementation, and Deployment of an IoT Based Smart Energy Management System. *IEEE Access* **2021**, *9*, 59649–59664. [[CrossRef](#)]

43. Huang, W.; Zhang, N.; Kang, C.; Li, M.; Huo, M. From demand response to integrated demand response: Review and prospect of research and application. *Prot. Control Mod. Power Syst.* **2019**, *4*, 12. [[CrossRef](#)]
44. Grisales-Noreña, L.F.; Montoya, O.D.; Cortés-Caicedo, B.; Zishan, F.; Rosero-García, J. Optimal Power Dispatch of PV Generators in AC Distribution Networks by Considering Solar, Environmental, and Power Demand Conditions from Colombia. *Mathematics* **2023**, *11*, 484. [[CrossRef](#)]
45. Mansouri, S.; Zishan, F.; Montoya, O.D.; Azimizadeh, M.; Giral-Ramírez, D.A. Using an intelligent method for microgrid generation and operation planning while considering load uncertainty. *Results Eng.* **2023**, *17*, 100978. [[CrossRef](#)]
46. Hajiamoosha, P.; Rastgou, A.; Bahramara, S.; Sadati, S.M.B. Stochastic energy management in a renewable energy-based microgrid considering demand response program. *Int. J. Electr. Power Energy Syst.* **2021**, *129*, 106791. [[CrossRef](#)]
47. Soroudi, A.; Keane, A. Risk averse energy hub management considering plug-in electric vehicles using information gap decision theory. In *Plug in Electric Vehicles in Smart Grids*; Springer: Singapore, 2015; pp. 107–127.
48. Doosti, R.; Sedighizadeh, M.; Sedighizadeh, D.; Sheikhi Fini, A. Robust stochastic optimal operation of an industrial building including plug in electric vehicle, solar-powered compressed air energy storage and ice storage conditioner: A case study in the city of Kaveh, Iran. *IET Smart Cities* **2022**, *4*, 56–77. [[CrossRef](#)]
49. Sedighizadeh, M.; Esmaili, M.; Jamshidi, A.; Ghaderi, M.-H. Stochastic multi-objective economic-environmental energy and reserve scheduling of microgrids considering battery energy storage system. *Int. J. Electr. Power Energy Syst.* **2019**, *106*, 1–16. [[CrossRef](#)]
50. Haghi, E.; Raahemifar, K.; Fowler, M. Investigating the effect of renewable energy incentives and hydrogen storage on advantages of stakeholders in a microgrid. *Energy Policy* **2018**, *113*, 206–222. [[CrossRef](#)]
51. Alayi, R.; Zishan, F.; Seyednouri, S.R.; Kumar, R.; Ahmadi, M.H.; Sharifpur, M. Optimal Load Frequency Control of Island Microgrids via a PID Controller in the Presence of Wind Turbine and PV. *Sustainability* **2021**, *13*, 10728. [[CrossRef](#)]
52. Zishan, F.; Akbari, E.; Montoya, O.D.; Giral-Ramírez, D.A.; Molina-Cabrera, A. Efficient PID Control Design for Frequency Regulation in an Independent Microgrid Based on the Hybrid PSO-GSA Algorithm. *Electronics* **2022**, *11*, 3886. [[CrossRef](#)]
53. Wang, D.; Tan, D.; Liu, L. Particle swarm optimization algorithm: An overview. *Soft Comput.* **2018**, *22*, 387–408. [[CrossRef](#)]
54. Mahdavi, M.; Fesanghary, M.; Damangir, E. An improved harmony search algorithm for solving optimization problems. *Appl. Math. Comput.* **2007**, *188*, 1567–1579. [[CrossRef](#)]

Disclaimer/Publisher’s Note: The statements, opinions and data contained in all publications are solely those of the individual author(s) and contributor(s) and not of MDPI and/or the editor(s). MDPI and/or the editor(s) disclaim responsibility for any injury to people or property resulting from any ideas, methods, instructions or products referred to in the content.